Journal of Mathematical Sciences, Vol. 180, No. 2, January, 2012

NUMERICAL SOLUTION OF THE PROBLEM OF THE STRESS-STRAIN STATE IN HOLLOW CYLINDERS USING SPLINE APPROXIMATIONS

A. Ya. Grigorenko,[1] **W. H. Müller,**[1,2] **R. Wille,**[1,2] **and S. N. Yaremchenko**[1,2]

UDC 539.3

The three-dimensional theory of elasticity is used for a study of the stress-strain state in a hollow cylinder with varying stiffness. The corresponding problem is solved by a method that is partly analytical and partly numerical in nature: Spline approximations and collocation are used to reduce the partial differential equations of elasticity to a boundary-value problem for a system of ordinary differential equations of higher order for the radial coordinate, which is then solved using the method of stable discrete orthogonalization. Results for an inhomogeneous cylinder for various types of stiffness are presented.

The increasingly stringent requirements for the estimation of strength characteristics, the tendency toward a detailed consideration of real properties of structural materials, and the discovery and study of three-dimensional effects occurring in thick-walled elements require the treatment of hollow cylindrical structures in terms of a three-dimensional model. Finding a solution for the stress-strain state in thick-walled structures within the framework of spatial linear elasticity theory goes hand-in-hand with significant difficulties related to the complexity of initial systems and partial differential equations, as well as the necessity of satisfying the boundary conditions prescribed on the surfaces of the elastic body. These difficulties arise substantially during the calculation of structural elements such as cylinders made of anisotropic and inhomogeneous materials. The facts mentioned above are consistent with the relative sparseness of the number of publications addressing such questions (Kollar, Patterson, and Springer [11], Banerjee and Henry [3], Kollar [10], Shi, Zhang, and Xiang [12], Gal and Dvorkin [5], Collin, Caillerie, and Chamlon [4], and Tsurkov and Drach [13]).

Along with universal approaches used for solving boundary-value problems in mechanics and mathematical physics, such as the finite-difference technique, finite-element method, and other discrete methods, the new technique now finds wide application for this particular class of problems [2, 3, 14]. It allows reducing the initial problem to a system of ordinary differential equations, based on an approximation of the solution with respect to other variables by analytical methods. The exact reduction of multidimensional problems to one-dimensional ones and the solution of the latter by the stable numerical method of discrete orthogonalization gives reasons to believe that the obtained results are highly accurate. Due to cylindrical geometry, the method of finite elements, if used for calculating the mechanical behavior, is time-consuming and inefficient and requires large memory and processing speed of the computer.

Recently, an approach based on spline approximations has been developed in several articles [6–9] in order to study the mechanical behavior of plate and shells. Its main advantages are the following [1]:

- stability against local perturbations, i.e., the local behavior of splines in the neighborhood of a point does not influence their overall behavior, in contrast to, e.g., the polynomial approximation;
- better convergence than that of the polynomial approximation;
- simple and convenient computer implementation.

[1] Timoshenko Institute of Mechanics, National Academy of Sciences of Ukraine, Kiev, Ukraine.

[2] Technical University of Berlin, Berlin, Germany.

Published in Matematychni Metody ta Fizyko-Mekhanichni Polya, Vol. 53, No. 3, pp. 127–134, July–September, 2010. Original article submitted March 5, 2010.

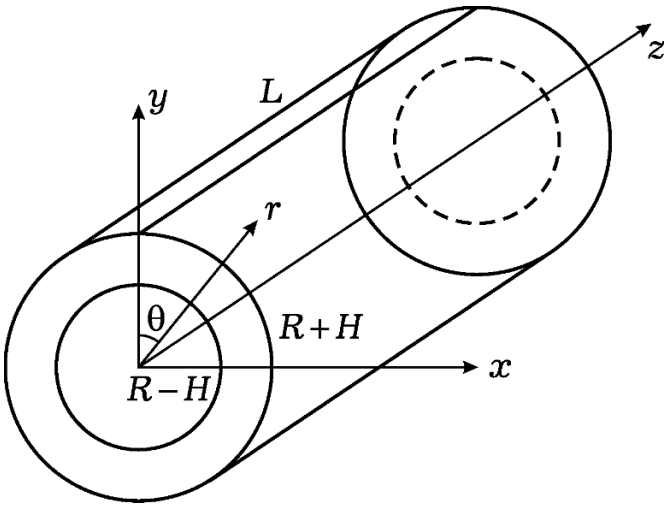

Fig. 1

The main goal of this article is the development of an efficient numerical-analytical approach to the solution of the problems of finding the stress-strain state states of hollow composite cylinders in a three-dimensional loading case. The proposed approach is a discrete–continuous one and is based on the combination of the spline-collocation method with the method of discrete orthogonalization. It allows reducing three-dimensional problems to one-dimensional ones and solving the latter by the stable numerical method of discrete orthogonalization with high degree of accuracy.

Basic Equations

We consider a hollow orthotropic cylinder of constant thickness (Fig. 1), inner radius $R-H$, outer radius $R+H$ (R is the radius of the mid-surface and $2H$ is the thickness of the cylinder), and length L described in a cylindrical coordinate system r, θ, z. The stress-strain state of this cylinder is described by the following equations of elasticity:

linear kinematic relations:

$$e_r = \frac{\partial u_r}{\partial r}, \qquad e_z = \frac{\partial u_z}{\partial z}, \qquad 2e_{rz} = \frac{\partial u_r}{\partial z} + \frac{\partial u_z}{\partial r}; \tag{1}$$

Hooke's law for a more general orthotropic case:

$$\sigma_r = \lambda_{11}e_r + \lambda_{12}e_\theta + \lambda_{13}e_z,$$

$$\sigma_\theta = \lambda_{12}e_r + \lambda_{22}e_\theta + \lambda_{23}e_z,$$

$$\sigma_z = \lambda_{13}e_r + \lambda_{23}e_\theta + \lambda_{33}e_z, \tag{2}$$

where the elements $\lambda_{ij} = \lambda_{ij}(r, z)$ of the stiffness matrix are continuous and differentiable functions of the coordinates r and z;

equations of equilibrium:

$$\frac{\partial \sigma_r}{\partial r} + \frac{\partial \sigma_{rz}}{\partial z} + \frac{\sigma_r - \sigma_\theta}{r} = 0, \qquad \frac{\partial \sigma_{rz}}{\partial r} + \frac{\partial \sigma_z}{\partial z} + \frac{\sigma_{rz}}{r} = 0; \tag{3}$$

here, $u_r(r,z)$ and $u_z(r,z)$ are the projections of the total displacement of the cylinder onto the tangents to the coordinate lines r and z, respectively, e_r, e_θ, and e_z are the relative linear strains along the coordinate lines, e_{rz} is the shear strain, σ_r, σ_θ, and σ_z are the normal stresses, and σ_{rz} is the tangential stress.

The elements λ_{ij} of the stiffness matrix follow from the elements c_{ij} of the compliance matrix as

$$\lambda_{11} = \left(\tilde{c}_{22}\tilde{c}_{33} - \tilde{c}_{23}^2\right)\frac{1}{\Delta}, \qquad \lambda_{12} = \left(\tilde{c}_{13}\tilde{c}_{23} - \tilde{c}_{12}\tilde{c}_{33}\right)\frac{1}{\Delta},$$

$$\lambda_{13} = \left(\tilde{c}_{12}\tilde{c}_{23} - \tilde{c}_{13}\tilde{c}_{22}\right)\frac{1}{\Delta}, \qquad \lambda_{22} = \left(\tilde{c}_{11}\tilde{c}_{33} - \tilde{c}_{13}^2\right)\frac{1}{\Delta},$$

$$\lambda_{23} = \left(\tilde{c}_{12}\tilde{c}_{13} - \tilde{c}_{11}\tilde{c}_{23}\right)\frac{1}{\Delta}, \qquad \lambda_{33} = \left(\tilde{c}_{11}\tilde{c}_{22} - \tilde{c}_{12}^2\right)\frac{1}{\Delta}, \quad \lambda_{55} = \frac{1}{c_{55}},$$

$$\Delta = c_{11}\left(c_{22}c_{33} - c_{23}^2\right) - c_{12}\left(c_{12}c_{33} - c_{13}c_{23}\right) + c_{13}\left(c_{12}c_{23} - c_{13}c_{22}\right). \tag{4}$$

In turn, the elements of the compliance matrix can be expressed in terms of the engineering constants:

$$c_{11} = \frac{1}{E_r}, \qquad c_{12} = -\frac{\nu_{r\theta}}{E_\theta}, \qquad c_{13} = -\frac{\nu_{rz}}{E_z},$$

$$c_{22} = \frac{1}{E_\theta}, \qquad c_{23} = -\frac{\nu_{\theta z}}{E_z}, \qquad c_{33} = \frac{1}{E_z}, \qquad c_{55} = -\frac{1}{G_{rz}}, \tag{5}$$

where E_r, E_θ, and E_z are the elastic moduli in the r-, θ-, and z-directions, respectively, G_{rz} is the shear modulus, and $\nu_{r\theta}$, ν_{rz}, and $\nu_{\theta z}$ are Poisson's ratios.

The boundary conditions on the internal $R-H$ and external $R+H$ surfaces of the cylinder are given by

$$\sigma_r(R-H,z) = 0, \qquad \sigma_r(R+H,z) = q, \qquad \sigma_{rz}(R \pm H,z) = 0. \tag{6}$$

We prescribe the following boundary conditions at the ends $z=0$ and $z=L$:

$$\text{(i)} \quad \sigma_r = 0, \quad u_r = 0 \quad \text{or} \quad \frac{\partial u_z}{\partial z} = 0, \quad u_r = 0; \tag{7}$$

(ii) $u_z = 0, \quad \sigma_{rz} = 0 \quad \text{or} \quad u_z = 0, \quad \dfrac{\partial u_r}{\partial z} = 0\,;$ (8)

(iii) $u_r = 0, \quad u_z = 0\,.$ (9)

The following system of equations for the displacements results:

$$\begin{aligned}
\frac{\partial^2 u_r}{\partial r^2} &= \left(-\frac{1}{\lambda_{11}}\frac{\partial \lambda_{12}}{\partial r}\frac{1}{r} + \frac{\lambda_{22}}{\lambda_{11}}\frac{1}{r^2}\right)u_r - \frac{1}{\lambda_{11}}\frac{\partial \lambda_{55}}{\partial z}\frac{\partial u_r}{\partial z} - \frac{\lambda_{55}}{\lambda_{11}}\frac{\partial^2 u_r}{\partial z^2} \\
&\quad - \left(\frac{1}{\lambda_{11}}\frac{\partial \lambda_{11}}{\partial r} + \frac{1}{r}\right)\frac{\partial u_r}{\partial r} - \left(\frac{1}{\lambda_{11}}\frac{\partial \lambda_{13}}{\partial r} - \frac{\lambda_{23} - \lambda_{13}}{\lambda_{11}}\frac{1}{r}\right)\frac{\partial u_z}{\partial z} \\
&\quad - \frac{1}{\lambda_{11}}\frac{\partial \lambda_{55}}{\partial z}\frac{\partial u_z}{\partial r} - \frac{\lambda_{13} + \lambda_{55}}{\lambda_{11}}\frac{\partial^2 u_z}{\partial z \partial r}\,, \\
\frac{\partial^2 u_z}{\partial r^2} &= -\frac{1}{\lambda_{55}}\frac{\partial \lambda_{23}}{\partial z}\frac{u_r}{r} - \left(\frac{1}{\lambda_{55}}\frac{\partial \lambda_{55}}{\partial r} + \frac{\lambda_{23}}{\lambda_{55}}\frac{1}{r} + \frac{1}{r}\right)\frac{\partial u_r}{\partial z} - \left(1 + \frac{\lambda_{13}}{\lambda_{55}}\right)\frac{\partial^2 u_r}{\partial r \partial z} \\
&\quad - \frac{1}{\lambda_{55}}\frac{\partial \lambda_{13}}{\partial z}\frac{\partial u_r}{\partial r} - \frac{1}{\lambda_{55}}\frac{\partial \lambda_{33}}{\partial z}\frac{\partial u_z}{\partial z} \\
&\quad - \frac{\lambda_{33}}{\lambda_{55}}\frac{\partial^2 u_z}{\partial z^2} - \left(\frac{1}{r} + \frac{1}{\lambda_{55}}\frac{\partial \lambda_{55}}{\partial r}\right)\frac{\partial u_z}{\partial r}\,.
\end{aligned} \tag{10}$$

We now reduce these equations to the form

$$\begin{aligned}
\frac{\partial^2 u_r}{\partial r^2} &= a_{11}u_r + a_{12}\frac{\partial u_r}{\partial z} + a_{13}\frac{\partial^2 u_r}{\partial z^2} + a_{14}\frac{\partial u_r}{\partial r} + a_{15}\frac{\partial u_z}{\partial z} + a_{16}\frac{\partial u_z}{\partial r} + a_{17}\frac{\partial^2 u_z}{\partial r \partial z}\,, \\
\frac{\partial^2 u_z}{\partial r^2} &= a_{21}u_r + a_{22}\frac{\partial u_r}{\partial z} + a_{23}\frac{\partial u_r}{\partial r} + a_{24}\frac{\partial^2 u_r}{\partial r \partial z} + a_{25}\frac{\partial u_z}{\partial z} + a_{26}\frac{\partial^2 u_z}{\partial z^2} + a_{27}\frac{\partial u_z}{\partial r}\,,
\end{aligned} \tag{11}$$

where the coefficients $a_{k\ell} = a_{k\ell}(r, z)$ are defined by

$$\begin{aligned}
a_{11} &= -\frac{1}{\lambda_{11}}\frac{\partial \lambda_{12}}{\partial r}\frac{1}{r} + \frac{\lambda_{22}}{\lambda_{11}}\frac{1}{r^2}\,, \qquad a_{12} = -\frac{1}{\lambda_{11}}\frac{\partial \lambda_{55}}{\partial z}\,, \\
a_{13} &= -\frac{\lambda_{55}}{\lambda_{11}}\,, \qquad a_{14} = -\left(\frac{1}{\lambda_{11}}\frac{\partial \lambda_{11}}{\partial r} + \frac{1}{r}\right),
\end{aligned}$$

$$a_{15} = -\left(\frac{1}{\lambda_{11}}\frac{\partial\lambda_{13}}{\partial r} - \frac{\lambda_{23}-\lambda_{13}}{\lambda_{11}}\frac{1}{r}\right), \qquad a_{16} = -\frac{1}{\lambda_{11}},$$

$$\frac{\partial\lambda_{55}}{\partial z}a_{17} = -\frac{\lambda_{13}+\lambda_{55}}{\lambda_{11}}, \qquad a_{21} = -\frac{1}{\lambda_{55}}\frac{\partial\lambda_{23}}{\partial z}\frac{1}{r},$$

$$a_{22} = -\left(\frac{1}{\lambda_{55}}\frac{\partial\lambda_{55}}{\partial r} + \frac{\lambda_{23}}{\lambda_{55}}\frac{1}{r} + \frac{1}{r}\right), \qquad a_{23} = -\frac{1}{\lambda_{55}}\frac{\partial\lambda_{13}}{\partial z},$$

$$a_{24} = -\left(1+\frac{\lambda_{13}}{\lambda_{55}}\right), \qquad a_{25} = -\frac{1}{\lambda_{55}}\frac{\partial\lambda_{33}}{\partial z},$$

$$a_{26} = -\frac{\lambda_{33}}{\lambda_{55}}, \qquad a_{27} = -\left(\frac{1}{r} + \frac{1}{\lambda_{55}}\frac{\partial\lambda_{55}}{\partial r}\right). \tag{12}$$

In this case, the boundary conditions (6) on the inner and outer surfaces become

$$\lambda_{11}\frac{\partial u_r}{\partial r} + \lambda_{12}\frac{u_r}{r} + \lambda_{13}\frac{\partial u_z}{\partial z} = 0, \qquad \lambda_{55}\left(\frac{\partial u_r}{\partial z} + \frac{\partial u_z}{\partial r}\right) = 0. \tag{13}$$

Solving Technique

The problem defined by Eq. (10) combined with appropriate boundary conditions can be solved by spline-collocation and discrete-orthogonalization methods. In preparation for the spline-collocation method, we write the unknown functions $u_r(r,z)$, $u_z(r,z)$ as follows:

$$u_r = \sum_{i=0}^{N} u_{ri}(r)\varphi_i^{(1)}(z), \qquad u_z = \sum_{i=0}^{N} u_{zi}(r)\varphi_i^{(2)}(z), \tag{14}$$

where $u_{ri}(r)$ and $u_{zi}(r)$ are sought functions of the variable r, and $\varphi_i^{(j)}(z)$, $j=1,2$, $i=0,1,\ldots,N$, are linear combinations of B-splines on the uniform mesh $\Delta: 0 = z_0 < z_1 < \ldots < z_N = L$ that must satisfy the boundary conditions at $z=0$ and $y=L$. System (10) includes derivatives of the unknown functions along the coordinate z of order no higher than 2. In this case, we may restrict ourselves to approximations of the third power, i.e.,

$$B_3^i(z) = \frac{1}{6}\begin{cases} 0, & -\infty < z < z_{i-2}, \\ y^3, & z_{i-2} \le z < z_{i-1}, \\ -3y^2+3y^2+3y+1, & z_{i-1} \le z < z_i, \\ 3y^3-6y^2+4, & z_i \le z < z_{i+1}, \\ (1-y)^3, & z_{i+1} \le z < z_{i+2}, \\ 0, & z_{i+2} \le z < \infty, \end{cases} \tag{15}$$

where $y = \dfrac{z - z_k}{h_z}$ on the interval $[z_k, z_{k+1}]$, $k = i-2, \ldots, i+1$, $i = -1, \ldots, N+1$, and $h_z = z_{k+1} - z_k = \text{const}$. In this case, the functions $\varphi_i^{(j)}(z)$ are as follows:

(1°) If the relevant resolving function (u_r or u_z) is equal to zero at $z = 0$ and $z = L$, then

$$\varphi_0{}^{(j)}(z) = -4B_3^{-1}(z) + B_3^0(z), \qquad \varphi_1{}^{(j)}(z) = B_3^{-1}(z) - \frac{1}{2}B_3^0(z) + B_3^1(z),$$

$$\varphi_i{}^{(j)}(z) = B_3^i(z), \qquad i = 2, 3, \ldots, N-2,$$

$$\varphi_{N-1}{}^{(j)}(z) = B_3^{N-1}(z) - \frac{1}{2}B_3^N(z) + B_3^{N+1}(z),$$

$$\varphi_N{}^{(j)}(z) = -4B_3^{N+1}(z) + B_3^N(z). \tag{16}$$

(2°) If the derivative with respect to the resolving function is equal to zero at $z = 0$ and $z = L$, then

$$\varphi_0{}^{(j)}(z) = B_3^0(z), \qquad \varphi_1{}^{(j)}(z) = B_3^{-1}(z) - \frac{1}{2}B_3^0(z) + B_3^1(z),$$

$$\varphi_{ji}(z) = B_3^i(z), \qquad i = 2, 3, \ldots, N-2,$$

$$\varphi_{N-1}{}^{(j)}(z) = B_3^{N-1}(z) - \frac{1}{2}B_3^N(z) + B_3^{N+1}(z), \qquad \varphi_N{}^{(j)}(z) = B_3^N(z). \tag{17}$$

(3°) If the relevant resolving function is equal to zero at $z = 0$ and the derivative of the resolving function with respect to z is also equal to zero at $z = L$, then

$$\varphi_0{}^{(j)}(z) = -4B_3^{-1}(z) + B_3^0(z), \qquad \varphi_1{}^{(j)}(z) = B_3^{-1}(z) - \frac{1}{2}B_3^0(z) + B_3^1(z),$$

$$\varphi_i{}^{(j)}(z) = B_3^i(z), \qquad i = 2, 3, \ldots, N-2,$$

$$\varphi_{N-1}{}^{(j)}(z) = B_3^{N-1}(z) - \frac{1}{2}B_3^N(z) + B_3^{N+1}(z), \qquad \varphi_N{}^{(j)}(z) = B_3^N(z). \tag{18}$$

Substituting Eqs. (14) into (10), we now require them to be satisfied at the specified collocation points $\xi_k \in [0, L]$, $k = 0, N$. We consider the case where the number of mesh nodes is even, i.e., $N = 2n+1$, $n \geq 3$. The selection of the collocation points $\xi_{2i} \in [z_{2i}, z_{2i+1}]$, $\xi_{2i+1} \in [z_{2i}, z_{2i+1}]$, $i = 0, 1, 2, \ldots, n$, in the form $\xi_{2i} = z_{2i} + s_1 h_z$, $\xi_{2i+1} = z_{2i} + s_2 h_z$, where $s_1 = 1/2 - \sqrt{3}/6$ and $s_2 = 1/2 + \sqrt{3}/6$ are the roots of the second-order Legendre polynomial, is optimal and essentially increases the degree of accuracy of the approxima-

tion. In this case, the number of collocation points is $\bar{N} = N+1$. As a result, we obtain a system of $4(N+1)$ linear differential equations for the functions u_{ri}, $\tilde{u}_{ri}$, u_{zi}, and $\tilde{u}_{zi}$, $i = 0,\dots,N$, where $u'_{ri} = \tilde{u}_{ri}$ and $u'_{zi} = \tilde{u}_{zi}$. Using the notation

$$\Phi_j = \left[\varphi_i^{(j)}(\xi_k)\right], \qquad k,i = 0,\dots,N, \quad j = 1,2,$$

$$\bar{u}_r = \{u_{r0}, u_{r1},\dots,u_{rN}\}^\top, \qquad \bar{\tilde{u}}_r = \{\tilde{u}_{r0}, \tilde{u}_{r1},\dots,\tilde{u}_{rN}\}^\top,$$

$$\bar{u}_z = \{u_{z0}, u_{z1},\dots,u_{zN}\}^\top, \qquad \bar{\tilde{u}}_z = \{\tilde{u}_{z0}, \tilde{u}_{z1},\dots,\tilde{u}_{zN}\}^\top,$$

$$\bar{a}_{k\ell}^\top = \{a_{k\ell}(r,\xi_0),\, a_{k\ell}(r,\xi_1),\dots,a_{k\ell}(r,\xi_N)\} \tag{19}$$

and representing the matrix $[c_i a_{ij}]$ in the form $\bar{c} * A$ for the matrix $A = [a_{ij}]$, $i,j = 0,\dots,N$, and vector $\bar{c} = \{c_0, c_1,\dots,c_N\}^\top$, we write the system of ordinary differential equations for u_{ri}, $\tilde{u}_{ri}$, u_{zi}, and $\tilde{u}_{zi}$ in the form

$$\frac{d\bar{u}_r}{dr} = \bar{\tilde{u}}_r,$$

$$\frac{d\bar{u}_z}{dr} = \bar{\tilde{u}}_z,$$

$$\frac{d\bar{\tilde{u}}_r}{dr} = \Phi_1^{-1}\left(\bar{a}_{11} * \Phi_1 + \bar{a}_{12} * \Phi_1' + \bar{a}_{13} * \Phi_1''\right)\bar{u}_r + \Phi_1^{-1}\left(\bar{a}_{14} * \Phi_1\right)\bar{\tilde{u}}_r$$
$$+ \Phi_1^{-1}(\bar{a}_{15} * \Phi_2')\bar{u}_z + \Phi_1^{-1}\left(\bar{a}_{16} * \Phi_2 + \bar{a}_{17} * \Phi_2'\right)\bar{\tilde{u}}_z,$$

$$\frac{d\bar{\tilde{u}}_z}{dy} = \Phi_2^{-1}\left(\bar{a}_{21}\Phi_1 + \bar{a}_{22}\Phi_1'\right)\bar{u}_r + \Phi_2^{-1}\left(\bar{a}_{23} * \Phi_1'\right)\bar{\tilde{u}}_r$$
$$+ \Phi_2^{-1}\left(\bar{a}_{24} * \Phi_2 + \bar{a}_{25} * \Phi_2' + \bar{a}_{26} * \Phi_2''\right)\bar{u}_z + \Phi_2^{-1}(\bar{a}_{27} * \Phi_2)\bar{\tilde{u}}_z, \tag{20}$$

which can be represented as

$$\frac{d\bar{Y}}{dr} = A(r)\bar{Y}, \qquad R - H \le r \le R + H, \tag{21}$$

where

$$\bar{Y} = \left\{u_{r0},\dots,u_{rN}, \tilde{u}_{r0},\dots,\tilde{u}_{rN}, u_{z0},\dots,u_{zN}, \tilde{u}_{z0},\dots,\tilde{u}_{zN}\right\}^\top$$

is a vector function depending on r, and $A(r)$ is a square matrix of the $4(N+1)\times 4(N+1)$ th order.

Boundary conditions for this system of ordinary differential equations are defined by

$$\bar{\lambda}_{11}\Phi_1\bar{\tilde{u}}_r + \bar{\lambda}_{12}\Phi_1\frac{1}{r}\bar{u}_r + \bar{\lambda}_{13}\Phi_2'\bar{u}_z = \bar{q}, \qquad \bar{\lambda}_{55}\Phi_1'\bar{u}_r + \bar{\lambda}_{55}\Phi_2\bar{\tilde{u}}_z = 0, \tag{22}$$

where

$$\bar{\lambda}_{1\ell}^{\top} = \{\lambda_{1\ell}(r,\xi_0),\lambda_{1\ell}(r,\xi_1),\ldots,\lambda_{1\ell}(r,\xi_N)\}, \qquad \ell = 1,2,3,$$

$$\bar{\lambda}_{55}^{\top} = \{\lambda_{55}(r,\xi_0),\lambda_{55}(r,\xi_1),\ldots,\lambda_{55}(r,\xi_N)\},$$

or by

$$B_1\bar{Y}(R-H) = \bar{b}_1, \qquad B_2\bar{Y}(R+H) = \bar{0}, \tag{23}$$

where B_1 and B_2 are rectangular matrices of the $2(N+1)\times 4(N+1)$th order and b_1 is the corresponding vector.

The boundary-value problem (21), (23) can be solved using a discrete-orthogonalization method.

Numerical Results

The modulus of elasticity E is supposed to vary along the radial coordinate r according to the power law

$$E(r) = \frac{E_0}{1+\alpha}\left(1+\alpha\left(\frac{r}{R-H}\right)^{\beta}\right). \tag{24}$$

The following parameters were used in context with the cylinder: $L=10$, $R=10$, $H=1$, and Poisson's ratio $\nu = 0.34$. The ends of the cylinder are clamped.

The dependences of the radial displacement $\hat{u}_r = u_r E_0/q$ and the circumferential stress $\hat{\sigma}_\theta = \sigma_\theta/q$ on the parameters used for the variation of Young's modulus [see Eq. (24)] are shown in Figs. 2–5 ($\alpha=1$ for varying values of β, and $\beta=1$ for varying values of α). The displacements and stresses in the middle section of the cylinder, i.e., at $z=L/2$, are shown for the inner surface for $r=R-H$ (solid lines), $r=R-H/2$ (dashed line), $r=R$ (dotted line), and $r=R+H/2$ (dashed-dotted line), and for the outer surface for $R=R+H$ (dashed-double dotted line).

The radial displacement $\hat{u}_r$ decreases when the parameter β increases from -5 to 5 (Fig. 2). The difference between the displacements on the inner and outer surfaces decreases as β increases.

Figure 3 shows that the circumferential stress $\hat{\sigma}_\theta$ on the inner surface decreases as β increases. On the outer surface, it behaves in the opposite way. In contrast to this, the stress in the mid-surface (when $r=R$) changes only slightly. Also, when β is negative, the circumferential stress on the inner surface is greater than on the outer surface, and vice versa for positive values of β.

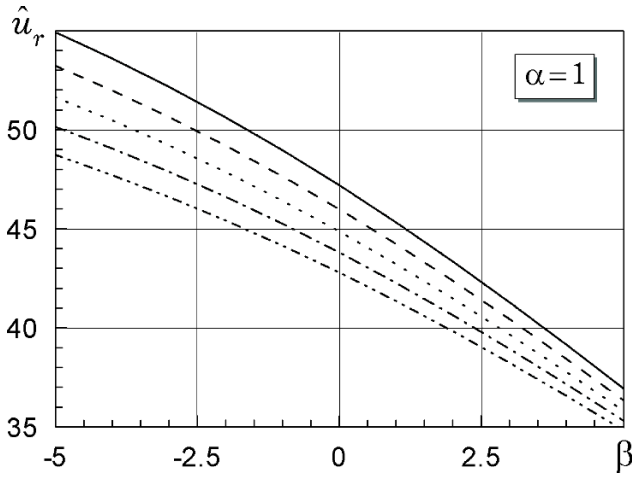

Fig. 2. Displacement $\hat{u}_r$ and its dependence on the parameter β.

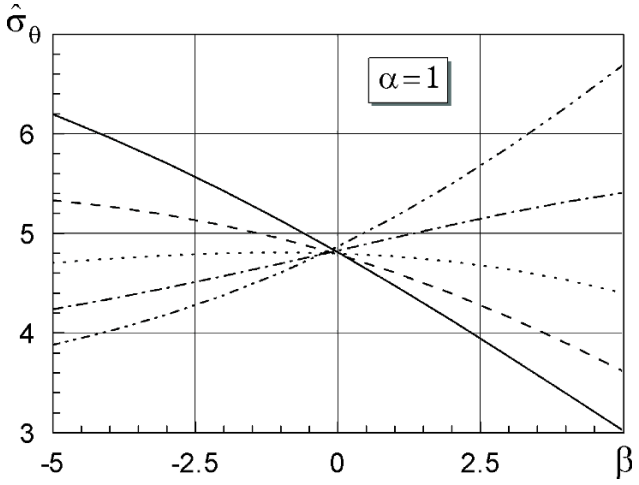

Fig. 3. Stress $\hat{\sigma}_\theta$ and its dependence on the parameter β.

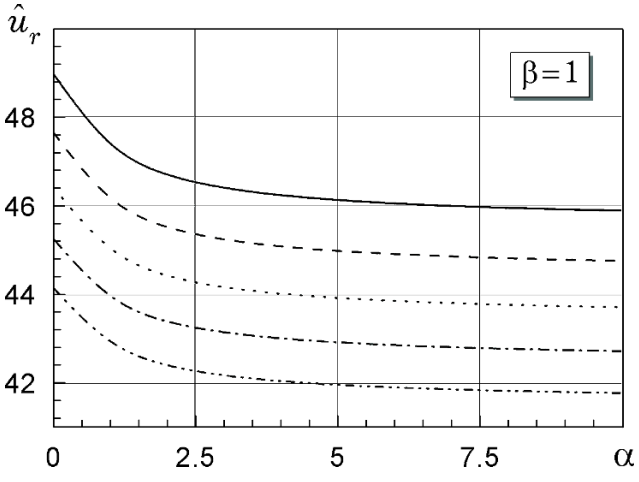

Fig. 4. Displacement $\hat{u}_r$ and its dependence on the parameter α.

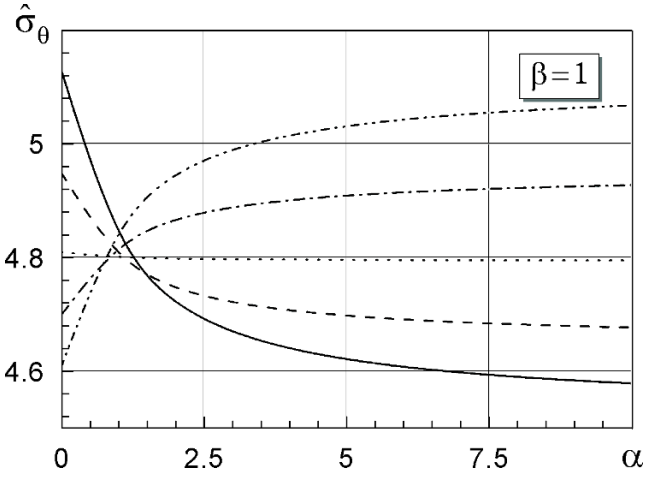

Fig. 5. Stress $\hat{\sigma}_\theta$ and its dependence on the parameter α.

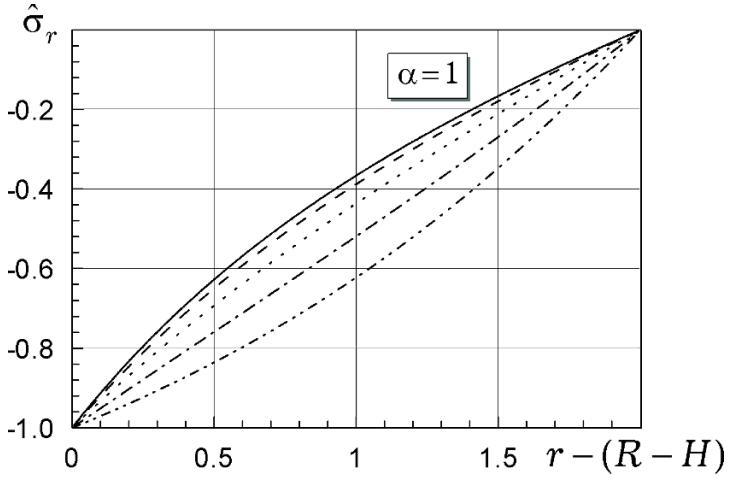

Fig. 6. Radial stress $\hat{\sigma}_\theta$ distribution as a function of radius r for various values of β.

It follows from Fig. 4 that the displacement $\hat{u}_r$ decreases as the parameter α increases from 0 to 10. The figure also shows that the greatest changes in the displacement occur within the interval $0 \le \alpha \le 5$, whereas for $5 \le \alpha \le 10$ the displacement varies only slightly. The same effect is observed in the case of the stress (Fig. 5). Moreover, the circumferential stress $\hat{\sigma}_\theta$ increases on the outer surface and decreases on the inner surface as α increases, exactly as in the case of β. Also, the maximum circumferential stress $\hat{\sigma}_\theta$ shifts from the inner surface to the outer one as α increases.

Figure 6 shows how the radial stress $\hat{\sigma}_r = \sigma_r / q$ varies from the inner to the outer cylinder surface in the middle section of the cylinder $(z = L/2)$, depending on the value of the parameter β. The following notation was used: solid line for $\beta = -10$, dashed line for $\beta = -5$, dotted line for $\beta = 0$, dashed-dotted line for $\beta = 5$, and dashed-double dotted line for $\beta = 10$ $(\alpha = 1)$. Predictably (as follows from the boundary conditions), the radial stresses on the inner and outer surfaces are -1 and 0, respectively. The curves change from concave to convex as β increases. The dependence of the stresses on the radius comes close to a straight line for $\beta = 5$.

Thus, by varying the physical parameters of the construction material, it is possible to influence the stress-strain distribution within the cylinder and to choose optimum parameters for its strength.

REFERENCES

1. J. H. Ahlberg, E. N. Nilson, and J. L. Walsh, *The Theory of Splines and Their Applications*, Academic Press, New York (1967).
2. I. Babuška, U. Banerjee, and J. E. Osborn, "Generalized finite element methods—main ideas, results and perspective," *Int. J. Comput. Methods*, **1**, 67–103 (2004).
3. P. K. Banerjee and D. P. Henry, "Elastic analysis of three-dimensional solids with fiber inclusions by BEM," *Int. J. Solids Struct.*, **29**, No. 20, 2423–2440 (1992).
4. F. Collin, D. Caillerie, and R. Chambon, "Analytical solutions for the thick-walled cylinder problem modeled with an isotropic elastic second gradient constitutive equation," *Int. J. Solids Struct.*, **46,** No. 22-23, 3927–3937 (2009).
5. D. Gal and J. Dvorkin, "Stresses in anisotropic cylinders," *Mech. Res. Commun.*, **22**, 109–113 (2009).
6. Ya. M. Grigorenko and S. N. Yaremchenko, "Refined analysis of the stress state of orthotropic elliptic cylindrical shells with variable geometrical parameters," *Int. Appl. Mech.*, **44**, No. 9, 998–1005 (2008).
7. A. Grigorenko and S. Yaremchenko, "Investigation of static and dynamic behavior of anisotropic inhomogeneous shallow shells by spline approximation method," *J. Civil Eng. Manag.*, **15**, No. 1, 87–93 (2009).
8. Ya. M. Grigorenko, A. Ya. Grigorenko, and L. I. Zakhairichenko, "Influence of geometrical parameters on the stress state of longitudinally corrugated elliptic cylindrical shells," *Int. Appl. Mech.*, **45**, No. 2, 187–192 (2009).
9. A. Ya. Grigorenko, N. P. Yaremchenko, and S. N. Yaremchenko, "Spline-based investigation of stress-strain state of anisotropic rectangular shallow shells of variable thickness in refined formulation," *J. Mech. Mater. Struct.* (Submitted in 2009).
10. L. P. Kollar, "Three-dimensional analysis of composite cylinders under axially varying hydrothermal and mechanical loads," *Comput. Struct.*, **50**, No. 4, 525–540 (1994).
11. L. P. Kollar, J. M. Patterson, and G. S. Springer, "Composite cylinders subjected to hydrothermal and mechanical loads," *Int. J. Solids Struct.*, **29**, No. 12, 1519–1534 (1992).
12. Z. Shi, T. Zhang, and H. Xiang, "Exact solution of heterogeneous elastic hollow cylinders," *Composite Struct.*, **79**, No. 1, 140–147 (2007).
13. I. Tsurkov and B. Drach, "Elastic deformation of composite cylinders with cylindrically orthotropic layers," *Int. J. Solids Struct.*, **47**, No. 1, 25–33 (2010).
14. O. C. Zienkiewicz and R. L. Taylor, *The Finite Element Method for Solid and Structural Mechanics*, Elsevier (2005).